Atmospheric Chemical Transport and Trajectory Modelling for Elevated Ozone Episodes and Climatological Patterns

Alexander Mahura [1], Roman Nuterman [1,2], Irina Petrova [2], Bjarne Amstrup [1]

[1] *Danish Meteorological Institute (DMI), Research Department, Lyngbyvej 100, Copenhagen, DK-2100, Denmark*
[2] *Tomsk State University, TSU, Lenin Ave., 36, 634050, Tomsk, Russia*
[3] *Russian State Hydrometeorological University, RSHU, Malookhtinskiy Prospekt, 98, 195196, St. Petersburg, Russia*

(Contact: E-mail: ama@dmi.dk; Phone: +45-3915-7423; Fax +45-3915-7400)

Times Series of Ozone Measurement

Among 9 Danish measurement sites, 3 sites (Figure 1) having long-term ozone measurement (with a time resolution of 1 hour and starting in early 1990s) records were selected – Ulborg (DK31; 56.28°N, 8.43°E) and Frederiksborg (DK32; 55.97°N, 12.33°E) and Lille Valby (DK41; 55.69°N, 12.13°E) located on Jutland Peninsula and Zealand Island of Denmark, respectively. These stations are operated by the National Environmental Research Institute (NERI, Denmark).

After pre-screening of the time series obtained from the European Monitoring and Evaluation Programme (EMEP) database at http://www.nilu.no/projects/ccc/emepdata.html (covering almost 15 year period and including almost 543 thousand valid observations), the measurements with high ozone level (using threshold as 150 µg/m^3) were selected accounting in total for 506 cases for these 3 locations. Among these, 42 (for DK41) and 59 (for DK31, and DK32) cases showed very high ozone concentrations (i.e. above 180 µg/m^3).

Figure 1. Danish measurement sites for ozone: DK31, 32, and 41.

Inter-Annual, Monthly & Diurnal Cycle Variability

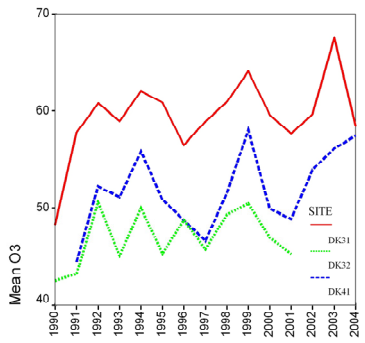

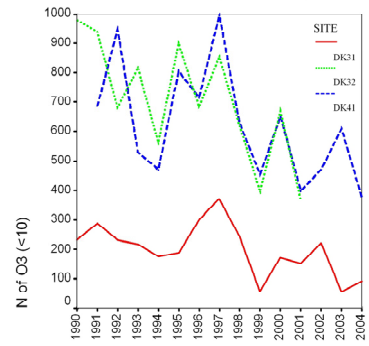

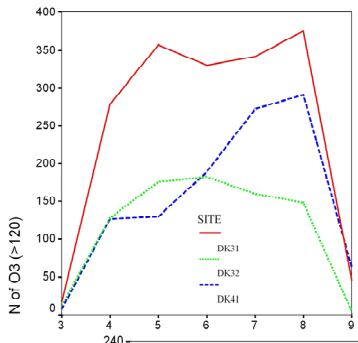

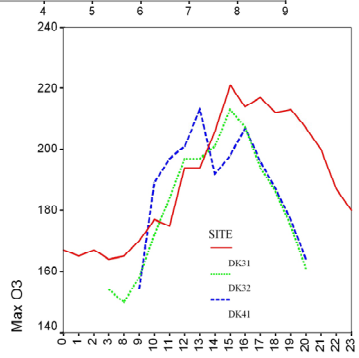

Figure 2.

Inter-Annual Variability
mean ozone concentration
(in µg/m^3)

Inter-Annual Variability
lower ozone concentration
(in µg/m^3)

Month-to-month variability
ozone concentration
more than 120 µg/m^3

Diurnal cycle
maximum ozone concentration
(in µg/m^3)

based on analysis
of the long-term time series
for 3 measurement stations.
(shown in Figure 1).

References

*Mahura A., Nuterman R., Petrova I., Amstrup B. (**2010**): Atmospheric Trajectory and Chemical Transport Modelling for Elevated Ozone Episodes.DMI Sci.Report, 10-05, 40p.*

*Draxler R.R., Rolph G.D. (**2003**): HYSPLIT (HYbrid Single-Particle Lagrangian Integrated Trajectory) Model access via NOAA ARL READY Website (http://www.arl.noaa.gov/ready/hysplit4.html). NOAA Air Resources Lab., Silver Spring, MD.*

*Gery, M.W., G.Z. Witten, J.P. Killus, M.C. Dodge (**1989**): A Photochemical Kinetics Mechanism for Urban and Regional Scale Computer Modeling. J. Geophys. Res., 94, 925-956.*

*Madronich, S. (**2002**): The prohospheric Visible Ultra-Violet (TUV) model webpage, National Center for Atmospheric Research, Boulder, CO. http://www.acd.edu/TUV/.*

*Rolph G.D. (**2003**): Real-time Environmental Applications and Display sYstem (READY) Website (http://www.arl.noaa.gov/ready/hysplit4.html). NOAA Air Resources Lab., Silver Spring, MD.*

*Sass, B.H., N.W. Nielsen, J.U. Jørgensen, B. Amstrup, M. Kmit and K.S. Mogensen (**2002**): The Operational DMI-HITLAM System -2002-version, DMI Tech. Rep., 99-21.*

*Stockwell, W.R., F. Kirchner, M. Kuhn, Seefeld, S. (**1997**): A New Mechanism for Regional Atmospheric Chemistry Modeling. J. Geophys. Res., 102, 25847-25879.*

Atmospheric Trajectory Modelling

For all these cases, at first, the trajectory modelling approach was applied in order to estimate atmospheric transport pathways of air mass arrival at the measurement sites and potential source regions from where the elevated ozone level can be associated. In our study the NOAA Hybrid Single Particle Lagrangian Integrated Trajectory Model (HYSPLIT; see at: http://www.arl.noaa.gov/ready/open/hysplit4.html; *Draxler & Rolph, 2003; Rolph, 2003*) model was used to calculate a set of backward trajectories (in total 506, with duration of 5 day backward in time and arriving at altitude of 100 m; examples are shown in Figure 3). Then, the clustering of trajectories was applied to divide these into groups with respect to potential source regions and dominating atmospheric transport pathways (summaries are given in Tables 1-2).

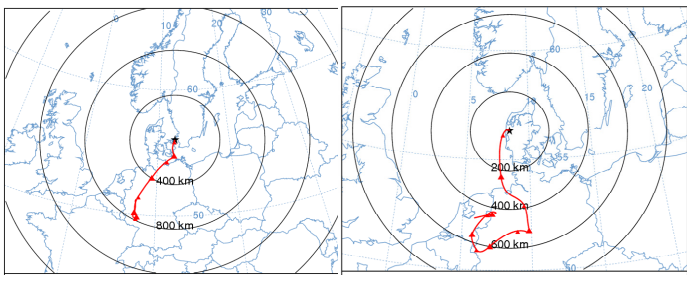

Figure 3. Backward trajectories (calculated by the NOAA HYSPLIT model) arriving (a) at DK32 station on 21 Jun 2000, 13 UTC; and (b) at DK31 on 6 Jun 1996, 18 UTC from the southern sector.

Sector	Pathway	Number of trajectories		
		DK31	DK32	DK41
E	*BST / RU — BSea — PL / GE*	25	16	30
SW	*AO — FR — Blux / GE*	12	11	20
S	*GE / Blux*	35	30	16
SE	*PL / GE*	14	31	23
NW	*AO — UK — Blux / GE*	25	23	20
	AO — NO — NSea	9	0	0
	AO — UK — NSea	27	7	6
	AO — Blux — GE	19	4	15
N	*Scand — BSea — PL / GE*	18	8	2
	Scand — BSea	9	7	10
NOID	*No clear identification*	14	2	18
Total (506 trajectories)		**207**	**139**	**160**

Table 1. Distribution of the number of trajectories associated with elevated ozone concentrations measured at the Danish sites as a function of the sector and pathway for the atmospheric transport /AO – Atlantic Ocean,
BSea — Baltic Sea, NSea — North Sea,
BST — Baltic States,
RU — Russia,
PL — Poland,
GE — Germany
FR — France,
Blux — Benelux countries
Scand. — from north of the Scandinavian countries (Norway/Sweden)/.

Sector	Pathway	% of trajectories		
		DK31	DK32	DK41
E	*BST / RU — BSea —PL / GE*	12.1	11.5	18.6
SW	*AO — FR — Blux / GE*	5.8	7.9	12.5
S	*GE / Blux*	16.8	21.6	10
SE	*PL / GE*	6.8	22.4	14.4
NW	*From AO —*	38.7	24.4	25.7
N	*From Scandinavia —*	13.1	10.8	7.5
NOID	*No clear identification*	6.7	1.4	11.3

Table 2. Percentage of trajectories associated with elevated ozone concentrations measured at the Danish sites as a function of the sector for the atmospheric transport.

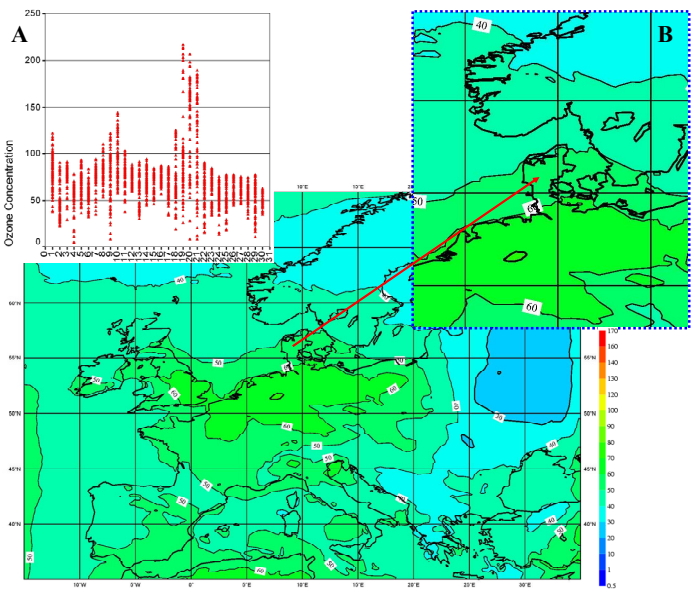

Figure 5. (A) Time-series of ozone measurement during June 2000 and (B) averaged monthly ozone concentration (in µg/m^3) for June 2000 (simulated by HIRLAM+CAMx).

Chemical Transport Modelling

Several relatively long-term episodes with continuous elevated ozone were identified in the analyzed time series; in particular, for DK31 – 7 episodes (having longest duration and observed in Jun 1996 and Jun 2000), DK32 – 5 (Jul 1992 and Jun 2000), and DK41 – 4 (Jul 1992 and Jun 2000).

For selected episodes the off-line Eulerian Chemistry-Aerosol-Cloud modeling system based on the HIRLAM (HIgh Resolution Limited Area Model) + CAMx (Comprehensive Air quality Model with extensions) had been run (in short-term and long-term modes) to simulate and evaluate in details patterns of atmospheric transport, dispersion, deposition, and transformation of ozone over the European domain.

See example in Figure 4 for June 2000). The monthly (June 2000) averaged ozone concentration field is shown in Figure 5. The seasonal (spring, summer, fall, and winter 2000) ozone concentration fields are shown in Figure 6.

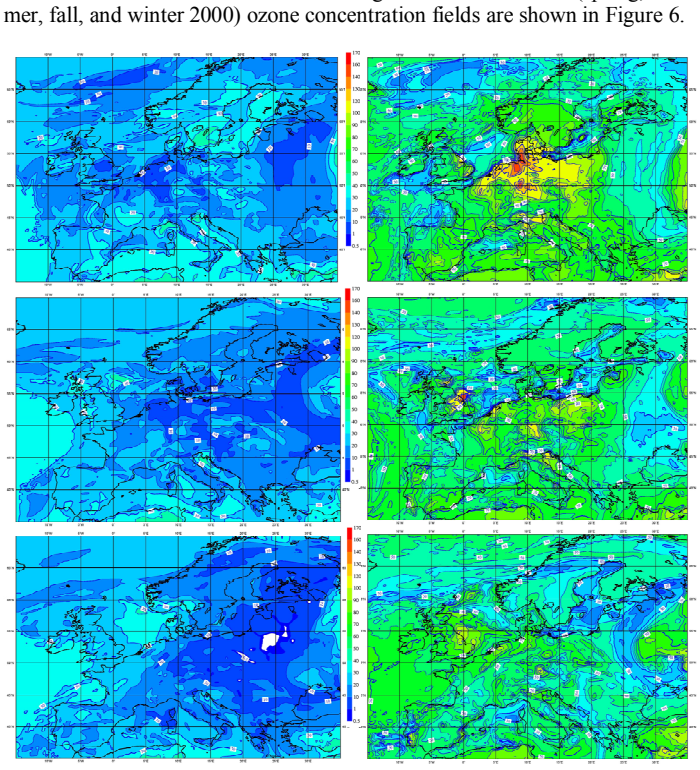

Figure 4. Ozone concentration (in µg/m^3) field for 19—20—21 Jun 2000 (at 12-right and 24—left UTC) (simulated by HIRLAM+CAMx).

This modeling system is a highly flexible multi-module based system. The module concept makes it easy to perform chemical transformations, and apply the model with other emission inventories and/or meteorological datasets.

In the present version two chemical schemes can be used: the Regional Acid Chemistry Mechanism (RACM) (*Stockwell et al., 1997*) and an updated version of Carbon Bond IV (CB-IV) Mechanism (*Gery et al., 1989*) with improved isoprene chemistry. Both mechanisms are used together with the Tropospheric Ultraviolet and Visible radiation model (TUV) (*Madronich, 2002*) to calculate photolysis rate coefficients, and emissions from EMEP.

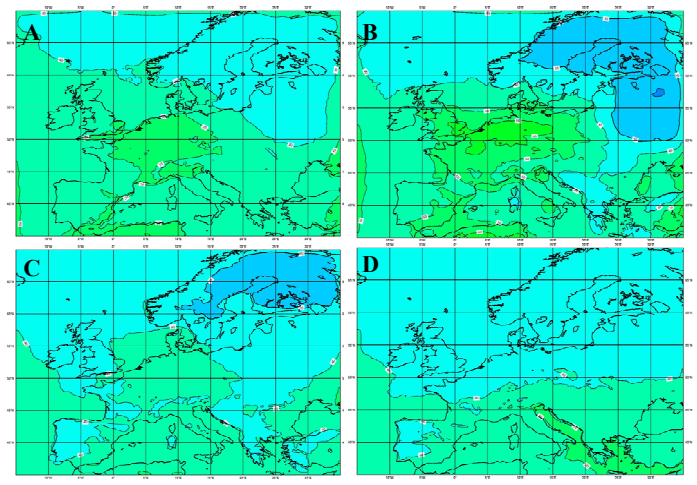

Figure 6. Averaged seasonal (A) spring, (B) summer, (C) fall, and (D) winter ozone concentration (in µg/m^3) for the year of 2000 (simulated by HIRLAM+CAMx).

As meteorological driver, the High Resolution Limited Area Model (HIRLAM) generated output with 3D meteorological fields are used. Different meteorological re-analysed archive datasets, from NWP such as DMI-HIRLAM (*Sass et al., 2002*) or ECMWF models or climate models can be used as meteorological driver for the modelling system.

At present, the following nested versions of the operational HIRLAM can be used as meteorological drivers for the modeling system:

T15 — 15 x 15 km, 40 vertical layers;
M09 — 9 x 9 km, 40 vertical levels;
S05 — 5 x 5 km, 40 vertical layers;
S03 — 3 x 3 km, 40 vertical levels.

The DMI-HIRLAM modelling system consists of the pre-processing, climate file generation, data-assimilation and analysis, initialization, forecast, post-processing, and verification. A forecast integration starts by assimilation of meteorological observations whereby a 3D state of the atmosphere is produced, which as well as possible is in accordance with the observations.